JPSE (Journal of Physical Science and Engineering), Vol. 9, No. 1, 2024, Page 20–28.
DOI: 10.17977/um024v9i12024p028

JPSE
(Journal of Physical Science and Engineering)

http://journal2.um.ac.id/index.php/jpse
EISSN: 2541-2485

Adsorption of Phosphate in Synthetic Laundry Wastewater using Empty Palm Oil Fruit Bunch

Received
1 January 2024

Revised
20 February 2024

Accepted for Publication
21 Maret 2024

Published
30 April 2024

I K Ariani*, E M Anifah, R Hudayarizka, and F Paramita

Department of Environmental Engineering, Institut Teknologi Kalimantan (ITK), Jl. Soekarno-Hatta Km.15, Karang Joang, Balikpapan, 76127, Indonesia.

***E-mail:** ismi.khairunnissa@lecturer.itk.ac.id

This work is licensed under a Creative Commons Attribution-ShareAlike 4.0 International License

Abstract

The laundry wastewater contains phosphates that can lead to eutrophication. Treatment of laundry wastewater with phosphate concentration can be done physically or chemically. The adsorption method was selected due to its high efficacy, and economical operation. Activated carbon derived from Empty Palm Oil Fruit Bunch (EPOFB) biomass waste was utilized as the adsorbent, leveraging its lignocellulosic components such as cellulose, hemicellulose, and lignin, that can adsorb pollutants. This study aims to assess the impact of adsorbent dosage and contact time on the adsorption capacity and phosphate removal efficiency. The activated carbon was produced from EPOFB via carbonization and activation processes at 400°C and KOH 6M. The variables including adsorbent dosage and contact time, ranging from 0.2 to 1.0 g/100mL and 20 to 100 minutes, respectively. Results indicate that the adsorbent dosage affects phosphate removal from synthetic laundry wastewater, while contact time does not significantly impact removal efficiency. The highest removal efficiencies of 67.37% and 70.03% were achieved at optimal doses of 8 g/L and 10 g/L, respectively, with contact times of 20 and 80 minutes. The isotherm model and kinetics of phosphate adsorption onto synthetic laundry wastewater using EPOFB adsorbent were identified as Freundlich and pseudo-second order, respectively.

Keywords: Activated carbon; Adsorption; EPOFB; Laundry wastewater; Phosphate

1. Introduction

Typically, a laundry facility utilizes 15 liters of water to process 1 kilogram of laundry and releases 400 m^3 of wastewater daily [1]. Detergent use contributes to surfactant levels ranging from 20-30% and phosphate levels between 70-80%. Phosphate primarily comes from Sodium Tripoly Phosphate (STPP), a key detergent component acting as a builder. Phosphate concentrations in laundry wastewater typically fall between 11-31 mg/L [2]. The presence of phosphate in STPP within laundry wastewater can promote the overgrowth of algae and cyanobacteria in aquatic environments, potentially triggering eutrophication. This process diminishes dissolved oxygen levels and the overall capacity of water bodies, leading to the demise of aquatic life [3].

Adsorption emerges as a viable method for phosphate removal from laundry wastewater due to its simplicity, cost-effectiveness, high efficacy, and lack of secondary pollution generation compared to chemical precipitation and ion-exchange methods. Studies have demonstrated the effectiveness of adsorption techniques in reducing phosphate levels using scallop shells as adsorbents [4]. Activated carbon stands out as a commonly employed adsorbent due to its capacity to adsorb both organic and inorganic substances [5]. Empty Palm Oil Fruit Bunch (EPOFB) represents one potential biomass source for activated carbon production.

EPOFB is solid waste from oil palm plantations, readily available and accounting for about 23% of the total fresh fruit bunches. The carbon content in EPOFB ranges from 40.93% to 68.3%. EPOFB contains lignocellulosic materials comprising 30–55% cellulose, 15–35% hemicellulose, and 20–30% lignin [6]. Lignocellulosic materials consist mainly of carbon, rendering them capable of adsorbing various pollutants. EPOFB has been utilized as an adsorbent in heavy metal adsorption processes, achieving an efficiency of 81.3% for Cu (II), and 99.56% for Cd [7]. Studies on the utilization of EPOFB

to reduce phosphate concentrations have not been widely conducted. Activation of activated carbon using acid or alkali solutions has also been carried out to enhance adsorption capacity. This study utilized activated carbon from EPOFB activated with KOH, which represents the novelty of this research.

2. Method

Method is a part consists of the design of the research, subject, instrument, data collection procedure, and data analysis.

2.1. Preparation of EPOFB activated carbon

EPOFB was taken from the oil plantations located in Muara Badak, Kutai Kartanegara District, Indonesia. EPOFB undergoes initial cutting and drying in an oven at 105°C for a duration of 24 hours. Following this, the material is subjected to carbonization at 400°C for 60 minutes [8]. After carbonization, the resulting charcoal is finely ground and sifted through a 100-mesh sieve [9]. The carbon derived from EPOFB undergoes chemical activation using a 6M KOH solution and is left to rest for 24 hours [10]. Subsequently, the activated carbon is thoroughly rinsed with distilled water and subsequently dried in an oven at 120°C for 1 hour [11].

2.2. Preparation of Synthetic Laundry Wastewater

The wastewater used is in the form of an artificial solution made from anhydrous potassium dihydrogen phosphate (KH_2PO_4). The phosphate concentration corresponds to the results of the characterization of laundry wastewater, which was taken from the wastewater outlet of a laundry business in North Balikpapan, Indonesia. The sampling was conducted using the grab sampling method in accordance with SNI 6989-59-2008.

Based on the characterization of the laundry wastewater, the initial phosphate concentration was 10 mg/L to determine the effect of varying adsorbent doses and contact time on phosphate removal efficiency. The use of synthetic waste is intended to make the research results more objective regarding the phosphate parameter.

$$Mass\ of\ {PO_4}^{-3} = \frac{Molecular\ weight\ KH_2PO_4}{Molecular\ weight\ PO_4} * [{PO_4}^{-3}] * Volume \quad (1)$$

Based on the above calculations, the procedure for preparing the KH_2PO_4 solution is as follows:

a. Weigh the grams of KH_2PO_4;
b. Place it in a 250 ml beaker glass and add 100 ml of distilled water;
c. Stir until homogeneous;
d. Transfer the resulting solution into a 1000 ml volumetric flask;
e. Dilute the solution with distilled water up to the mark and shake until homogeneous;
f. The KH_2PO_4 solution is obtained.

2.3. Preparation of Activator Solution KOH 6M

To dissolve KOH, this equation is used.

$$Molarity = \frac{Mass\ of\ KOH}{Molecular\ weight\ KOH} * \frac{1000}{Volume} \quad (2)$$

2.4. Characterization of Activated Carbon

The characterization of activated carbon is conducted by examining the moisture content, ash, and fixed carbon in EPOFB activated carbon, as shown in Table 1.

Table 1. Methods of examination for activated carbon characterization

Parameter	Unit	Methods of Examination	Formula
Moisture content	%	ASTM D-3173-03 [12]	$\frac{mass\ of\ crucible + mass\ of\ activated\ carbon\ (gram)}{mass\ of\ crucible\ (gram)}$
Ash content		ASTM D-3174-04 [13]	$\frac{mass\ of\ crucible + mass\ of\ activated\ carbon\ (gram)}{mass\ of\ activated\ carbon\ (gram)}$
Fixed carbon		ASTM D-3173-07 [14]	$100\% - (moisture\ content + volatile\ matter + ash\ content)$

Subsequently, the results of these characteristics are compared with the quality standards for activated carbon as per SNI 06-3730-1995. The tools used for activated carbon characterization are porcelain crucible (as a container for EPOFB samples), oven (to remove the moisture content [15] and ash content from EPOFB biomass at 105℃ for 1 and 2 hour, respectively), furnace 950℃ (for ash content examination), desiccator (for drying samples under atmospheric pressure or vacuum pressure), and an analytical balance (to measure the mass of an object precisely).

Following this procedure, FTIR testing was carried out to analyze the surface morphology and functional groups of the activated carbon. FTIR analysis was conducted in Integrated Laboratory in Institut Teknologi Kalimantan, Indonesia. FTIR was performed before and after activation process within the wavenumber range of 400 cm^{-1} to 4000 cm^{-1}. After that, BET test was conducted and aimed to measure the surface area and pore volume of the carbon before and after activation.

2.5. Adsorption Process

The adsorption process is carried out using a batch system with a 50 ml synthetic wastewater placed in a 250 mL Erlenmeyer flask at room temperature of 20-25°C, with pH measured before and after the treatment. The pH is adjusted to neutral by adding 0.1 M HCl and 0.1 M NaOH solutions. This study is conducted with treatments according to the research variables in Table 2 below.

Table 2. Research variables

		Adsorbent Dosage (g/50 mL)				
		0.1	0.2	0.3	0.4	0.5
Contact time (minute)	20	0.1 ; 20	0.2 ; 20	0.3 ; 20	0.4 ; 20	0.5 ; 20
	40	0.1 ; 40	0.2 ; 40	0.3 ; 40	0.4 ; 40	0.5 ; 40
	60	0.1 ; 60	0.2 ; 60	0.3 ; 60	0.4 ; 60	0.5 ; 60
	80	0.1 ; 80	0.2 ; 80	0.3 ; 80	0.4 ; 80	0.5 ; 80
	100	0.1 ; 100	0.2 ; 100	0.3 ; 100	0.4 ; 100	0.5 ; 100

The stirring speed used is 100 rpm [16]. Next, filtering with Whatman No. 42 filter paper is employed to separate the adsorbent and filtrate. After the samples are separated, they are measured to determine the final pH value and phosphate concentration in the filtrate.

2. Result and Discussion

2.1. Proximate Analysis

Based on the research results, the moisture content value of EPOFB activated carbon is 0.58%. This moisture content value has met the SNI 06-3730-1995 standard, which is below 10%. The low moisture content in activated carbon can also be caused by the hygroscopic nature of the 6M KOH activator. Volatile matter testing aims to determine non-carbon compounds. High carbonization temperature results in the evaporation of volatile matter [17]. The volatile matter content in EPOFB activated carbon is 11.79%. The ash content in EPOFB activated carbon is 10.48%. This ash content value has not met the required standard, which is below 10%. The ash content value can be influenced by mineral content such as Ca, K, Mg, and Na in activated carbon [18]. The high ash content causes pore blockage, reducing the adsorption capacity of activated carbon [19].

Fixed carbon content is the amount of pure carbon present in EPOFB activated carbon. The fixed carbon content in EPOFB activated carbon is 77.05%. This fixed carbon content value has met the required standard, which is above 60%. This is related to the characteristics of EPOFB, which contain a carbon content of 40.93-68.3% [20]. Additionally, EPOFB contains lignocellulosic materials consisting of cellulose ($C_6H_{10}O_5$), hemicellulose ($C_5H_8O_4$), and lignin ($C_{81}H_{92}O_{28}$) [21]. These lignocellulosic materials can be degraded into simple carbon chains through pyrolysis at temperatures of 300-600°C. Similar results were also found in previous studies on the fixed carbon content in EPOFB activated by H_3PO_4, which was 75% [17].

2.2. FTIR Analysis

Based on the test results, the wave number of 3025.50 cm^{-1} indicates the presence of C-C groups from aromatic compounds. The C-C groups were identified in the range of 3010-3100 cm^{-1}. In the absorption peak of the CC group, stretching occurs, resulting in the absorption peak being unidentifiable after activation. the formation of O-H groups after activation are detected at wave number of 3365.85 cm^{-1}.

Previous research indicated that O-H groups were present in the range of 3500–3200 cm^{-1} [22]. New peaks, identified as C-O groups, appear at the wave number of 1258.22 cm^{-1}, falling within the range of 1340-1470 cm^{-1}. The absorption peak of the C=C group shifts from 1555.44 cm^{-1} to 1573.47 cm^{-1}. The C=C groups are present in the range of 1500-1400 cm^{-1}. Shifts are also found in the range of 695-995 cm^{-1}, indicating the presence of C-H groups at absorption wave numbers of 994.57 cm^{-1} and 866.83 cm^{-1}. The shift in wave absorption indicates that the C=C and C-H groups undergo bending vibration (bonding) characterized by peak narrowing. Based on Figure 1, it can be concluded that the adsorbent has functional groups with a typical activated carbon structure containing O-H, C-O, C-C, and aromatic C=C and C-H groups used as active groups to adsorb adsorbates.

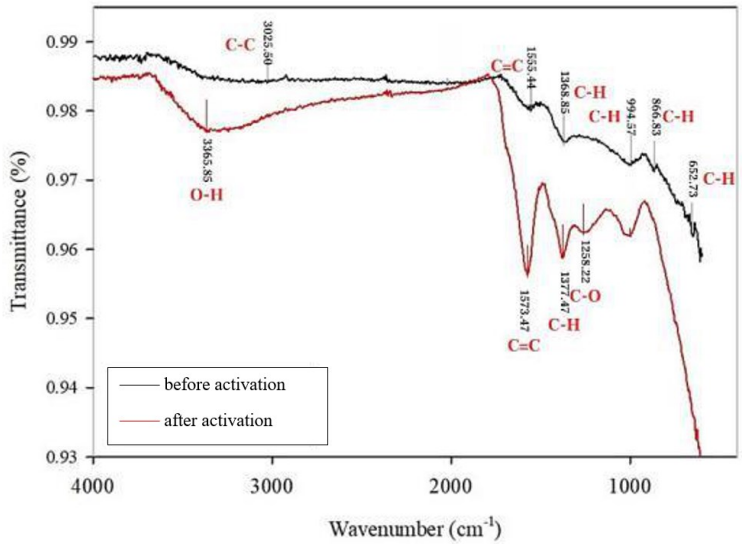

Figure 1. FTIR analysis of EPOFB activated carbon

2.3. BET Analysis

The surface area of carbon after activation is 224.513 m^2/g. The surface area of activated carbon is larger compared to before activation, which was 0.26 m^2/g. In previous research, an increase in surface area after activation was found, from 2.34 m^2/g to 263 m^2/g [8]. Additionally, there was an increase in pore volume after activation, from 0.0039 cm^3/g to 0.1653 cm^3/g. This can occur because activation can increase surface area through the binding of H_2O molecules and reducing tar formation. The increase in surface area is also due to the increased formation of micropores, which are <2 nm in size. The formation of micropores is indicated by a decrease in pore diameter after activation, from 15.15 nm to 1.1 nm. Activation results in the formation of a microporous structure in EPOFB activated carbon.

2.4. The Impact of Adsorbent Dosage on Phosphate Removal Efficiency and Adsorption Capacity

Figure 2 shows that as the adsorbent dosage increases, the phosphate removal efficiency also increases. At dosages ranging from 2 g/L to 8 g/L, the phosphate removal efficiency increases from 52.08% to 70.03%. The addition of adsorbent dosage can increase the surface area and active sites, allowing for more adsorbate to be absorbed. However, at a dosage of 10 g/L and a contact time of 20 minutes, there is a decrease in removal efficiency from 67.37% to 54.94%. This decrease occurs when the addition of dosage exceeds the optimum dosage, resulting in the accumulation of adsorbent particles. This condition leads to hindrance in the bulk transfer stage between the adsorbent and adsorbate, thus reducing the adsorbent's adsorption capacity. Based on the results shown in Figure 2, the optimum dosage of EPOFB activated carbon is 8 g/L and 10 g/L with removal efficiencies of 67.37% and 70.03%, respectively.

The addition of dosage from 2 g/L to 10 g/L results in a decrease in adsorption capacity from 2.64 mg/g to 0.71 mg/g, as shown in Figure 3. The highest adsorption capacity is found at a dosage of 2 grams, which is 2.64 mg/g. This high adsorption capacity indicates the optimum dosage of EPOFB activated carbon, suggesting that the adsorbent's active sites have maximally absorbed phosphate. The decrease in adsorption capacity occurs at a dosage of 10 grams with a capacity of 0.56 mg/g. The

decrease in adsorption capacity can be attributed to the competition between cations for the adsorption sites of adsorbent particles, leading to the closure of active sites on the surface of adsorbent [23].

The statistical analysis used was parametric analysis with the one-way ANOVA method. Based on the results of the normality test, significance values > 0.05 were obtained, indicating that the data were normally distributed. The results obtained from the homogeneity test indicated significance values > 0.05, suggesting that the data obtained were homogeneous. Regarding the use of dosage variations, the significance value was 0.001, meaning that the dosage variations of the adsorbent had a significant effect on phosphate removal efficiency in synthetic laundry wastewater.

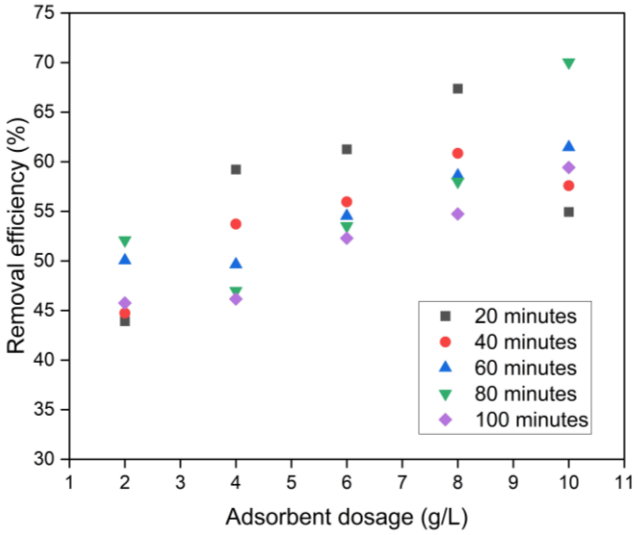

Figure 2. Impact of adsorbent dosage on the removal efficiency

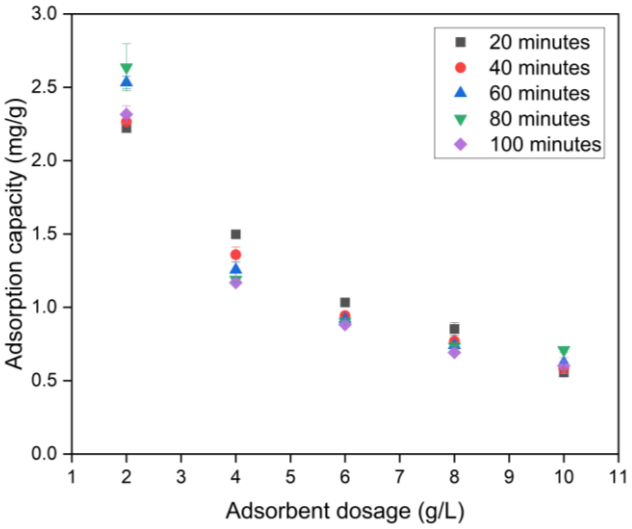

Figure 3. Impact of adsorbent dosage on the adsorption capacity

2.5. The Impact of Contact Time on Phosphate Removal Efficiency and Adsorption Capacity

In Figure 4, within the adsorbent dosage range of 4-8 g/L, an increase in contact time results in a decrease in efficiency. At contact times ranging from 20 to 100 minutes, there is a decrease in phosphate removal efficiency from 67.37% to 54.73%. This indicates a reduction in active sites due to adsorbent particles binding with phosphate [24]. The interaction between adsorbent and adsorbate leads to the formation of a layer on the adsorbent's surface, thereby covering it. Increased contact time leads to desorption. However, contrary to previous results, at dosages of 2 g/L and 10 g/L, an increase in contact time from 20 to 80 minutes results in an increase in removal efficiency from 54.94% to 70.03%.

Increased contact time can enhance the interaction of phosphate with empty active sites, resulting in increased adsorbate uptake [25]. Meanwhile, at a contact time of 100 minutes, there is a decrease in phosphate removal efficiency from 70.03% to 59.42%. This decrease indicates that the adsorbent has reached saturation, resulting in repulsive forces between adsorbate molecules and the adsorbent. Based on the results, the optimum contact time for EPOFB activated carbon is 20 and 80 minutes, with removal efficiencies of 67.37% and 70.03%, respectively.

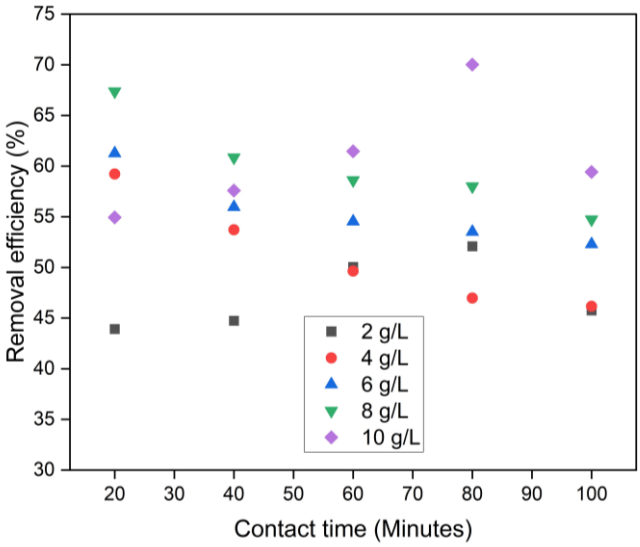

Figure 4. Impact of contact time on the removal efficiency

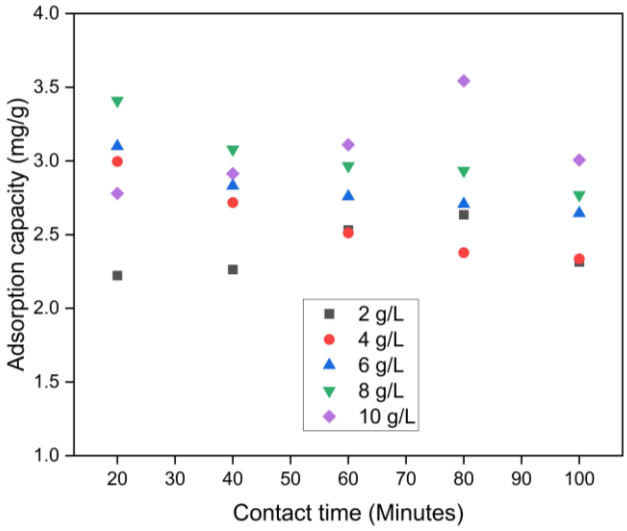

Figure 5. Impact of contact time on the adsorption capacity

Figure 5 shows that contact time does not significantly affect the adsorption capacity for phosphate. A contact time of 20 minutes demonstrates high adsorption capacity for all dosage variations. This indicates abundant availability of active sites, leading to increased adsorbent adsorption capacity [25]. At a contact time of 20 minutes, the initial phosphate adsorption capacity is 2.26 mg/g. Meanwhile, at 80 minutes, equilibrium time is reached for dosages of 2 g/L and 10 g/L. This occurs because the availability of active sites affects phosphate adsorption capacity. Dosages of 2 g/L and 10 g/L have fewer active sites compared to dosages of 4, 6, and 8 g/L, triggering less adsorption capacity [26]. Additionally, a dosage of 10 g/L experiences adsorbent agglomeration, resulting in reduced active site availability.

The decrease in adsorption capacity is also related to the large size of phosphate molecules, requiring more time to achieve bond stability on the adsorbent surface. Finally, at the last contact time

of 100 minutes, the phosphate adsorption capacity decreases to 1.17 mg/g because the adsorbent has reached equilibrium [27]. As for the statistical analysis of contact time variations, the significance value was 0.717, indicating that contact time variations did not have a significant effect on phosphate removal efficiency in synthetic laundry wastewater.

2.6. Isotherm Analysis and Adsorption Kinetics

The equations and parameters of Freundlich and Langmuir isotherms are shown in Table 3. Isotherm modeling was conducted at a contact time of 40 minutes with varying dosages. Based on the isotherm analysis results, the correlation coefficient (R^2) of the Freundlich isotherm (0.817) is closer to 1 compared to the Langmuir isotherm (0.561). Based on the isotherm modeling, phosphate adsorption using EPOFB activated carbon follows the Freundlich isotherm model. Previous studies using coal stove ash waste and acidic soil in Kenya for phosphate adsorption also reported that the isotherm model follows the Freundlich isotherm [28][29]. The Freundlich isotherm model describes the adsorption process occurring by forming non-uniform layers on the adsorbent surface [30]. The parameter 1/n, indicating the surface heterogeneity of the adsorbent, is 3.702. A value of $1/n > 1$ indicates low affinity between the adsorbate and adsorbent at low concentrations due to competition between water molecules and phosphate for adsorption on activated carbon.

The coefficients of pseudo first-order and pseudo second-order adsorption kinetics for phosphate adsorption using EPOFB activated carbon at the optimum dosage of 8 g/L are shown in Table 3. The correlation coefficient (R^2) value for pseudo second-order kinetics, namely 0.99, is closer to one than that for pseudo first-order kinetics. This proves that the phosphate adsorption process in synthetic laundry wastewater is described by pseudo second-order kinetics. Pseudo second-order kinetics indicate that adsorption with EPOFB activated carbon occurs due to covalent bonding between the adsorbent and adsorbate through electron sharing or exchange [31]. Phosphate can be trapped on different surfaces of the adsorbent based on pseudo second-order adsorption kinetics [32]. Phosphate absorption rate following pseudo-order kinetics has also been reported in phosphate adsorption studies using activated carbon from peanut shells [33] and date palm fiber bioadsorbents. The adsorption capacity based on pseudo second-order kinetics calculation is 0.67 mg/g, while for pseudo first-order kinetics, it is 2.14 mg/g. The adsorption capacity value based on pseudo second-order kinetics is closer to the experimental adsorption capacity value of 0.85 mg/g.

Table 3. Isotherm Analysis and Adsorption Kinetics

Freundlich		Langmuir	
Equation	y = 3.702x – 2.4187	Equation	y = 2.2647x + 15.042
R^2	0.817	R^2	0.561
K_f	262.240	q_m	0.442
1/n	3.702	K_L	0.4416
n	0.2701		
Adsorption kinetics result			
Pseudo first-order		Pseudo second-order	
R^2	0.26	R^2	0.99
Q_e exp (mg/g)	0.85	Q_e exp (mg/g)	0.85
Q_e cal (mg/g)	2.14	Q_e cal (mg/g)	0.67
K_1 (/menit)	0.003	K_1 (/menit)	0.29
		h (mg/g.menit)	0.1225

3. Conclusion

The dosage of EPOFB adsorbent affects phosphate removal in synthetic laundry wastewater. Meanwhile, contact time does not significantly affect phosphate removal efficiency. The highest removal efficiency of 67.37% and 70.03% was achieved at the optimum dosages of 8 g/L and 10 g/L with contact times of 20 and 80 minutes, respectively. The isotherm and kinetic models for phosphate adsorption in synthetic laundry wastewater using EPOFB adsorbent are Freundlich and pseudo-second-order kinetics.

Acknowledgment

The author would like to express gratitude to BIMA Kemdikbudristek for funding this research under the scope of the Junior Faculty Research Grant (*Ruang Lingkup Penelitian Dosen Pemula*).

References

[1] S. M. Mohan, "Use of naturalized coagulants in removing laundry waste surfactant using various unit processes in lab-scale," *J. Environ. Manage.*, vol. 136, pp. 103–111, 2014, doi: 10.1016/j.jenvman.2014.02.004.

[2] A. Damayanti and T. Kumala Sari, "The Performance Operation of Zeolite as Membrane with using Laundry Waste Water," *J. Membr. Sci. Technol.*, vol. 6, no. 2, 2016, doi: 10.4172/2155-9589.1000148.

[3] S. S. Rathore, P. Chandravanshi, A. Chandravanshi, and K. Jaiswal, "Eutrophication: Impacts of Excess Nutrient Inputs on Aquatic Ecosystem," *IOSR J. Agric. Vet. Sci.*, vol. 09, no. 10, pp. 89–96, 2016, doi: 10.9790/2380-0910018996.

[4] H. Bacelo, A. M. A. Pintor, S. C. R. Santos, R. A. R. Boaventura, and C. M. S. Botelho, "Performance and prospects of different adsorbents for phosphorus uptake and recovery from water," *Chem. Eng. J.*, vol. 381, no. June 2019, p. 122566, 2020, doi: 10.1016/j.cej.2019.122566.

[5] M. M. Sabzehmeidani, S. Mahnaee, M. Ghaedi, H. Heidari, and V. A. L. Roy, "Carbon based materials: A review of adsorbents for inorganic and organic compounds," *Mater. Adv.*, vol. 2, no. 2, pp. 598–627, 2021, doi: 10.1039/d0ma00087f.

[6] M. Faisal, A. Gani, and Z. Fuadi, "Utilization of Activated Carbon From Palm Kernel Shells As the Bioadsorbent of Lead Waste," *Int. J. GEOMATE*, vol. 20, no. 78, pp. 81–86, 2021, doi: 10.21660/2021.78.6135.

[7] B. C. Ekeoma, N. S. Sambudi, and C. O. Ndukwe, "Activated Empty Palm Fruit Bunch for the Adsorption of Heavy Metal Ions: Kinetics and Thermodynamics," *Phys. Chem. Res.*, vol. 10, no. 4, pp. 505–518, 2022, doi: 10.22036/PCR.2022.319988.2002.

[8] D. A. Munar-Florez, D. A. Varón-Cardenas, N. E. Ramírez-Contreras, and J. A. García-Núñez, "Adsorption of ammonium and phosphates by biochar produced from oil palm shells: Effects of production conditions," *Results Chem.*, vol. 3, no. June 2020, p. 100119, 2021, doi: 10.1016/j.rechem.2021.100119.

[9] M. Yang, J. Lin, Y. Zhan, and H. Zhang, "Adsorption of phosphate from water on lake sediments amended with zirconium-modified zeolites in batch mode," *Ecol. Eng.*, vol. 71, pp. 223–233, 2014, doi: 10.1016/j.ecoleng.2014.07.035.

[10] H. Tran Thi Dieu, K. Charoensook, H. C. Tai, Y. T. Lin, and Y. Y. Li, "Preparation of activated carbon derived from oil palm empty fruit bunches and its modification by nitrogen doping for supercapacitors," *J. Porous Mater.*, vol. 28, no. 1, pp. 9–18, 2021, doi: 10.1007/s10934-020-00957-2.

[11] S. Li, K. Han, J. Li, M. Li, and C. Lu, "Preparation and characterization of super activated carbon produced from gulfweed by KOH activation," *Microporous Mesoporous Mater.*, vol. 243, pp. 291–300, 2017, doi: 10.1016/j.micromeso.2017.02.052.

[12] U. Shafiq, "Proximate Analysis of Low and High Quality Pure Coal and their Blends from Pakistan," *Austin Chem. Eng.*, vol. 4, no. 1, pp. 1–3, 2017, doi: 10.26420/austinchemeng.2017.1048.

[13] Suliestyah, E. J. Tuheteru, R. Yulianti, C. Palit, C. C. Yomaki, and S. N. Ahmad, "Production of activated carbon from coal with H3PO4 activation for adsorption of Fe(II) and Mn(II) in acid mine drainage," *J. Degrad. Min. Lands Manag.*, vol. 11, no. 3, pp. 5755–5765, 2024, doi: 10.15243/jdmlm.2024.113.5755.

[14] K. Q. Tran, M. Z. Alonso, L. Wang, and Ø. Skreiberg, "Simultaneously Boosting the Mass and Fixed-carbon Yields of Charcoal from Forest Residue via Atmospheric Carbonization," *Energy Procedia*, vol. 105, no. May, pp. 787–792, 2017, doi: 10.1016/j.egypro.2017.03.390.

[15] R. Desiasni, F. Widyawati, Y. Sersaningsih, S. Bahtiar, and A. Kusmiran, "Physical and Mechanical Properties of Fiber Board from Corn Husk Fiber," *JPSE (Journal Phys. Sci. Eng.*, vol. 7, no. 2, pp. 134–141, 2022, doi: 10.17977/um024v7i22022p134.

[16] K. Kuśmierek and A. ̄wia¸tkowski, "The influence of different agitation techniques on the adsorption kinetics of 4-chlorophenol on granular activated carbon," *React. Kinet. Mech. Catal.*, vol. 116, no. 1, pp. 261–271, 2015, doi: 10.1007/s11144-015-0889-1.

[17] S. Maulina and M. Iriansyah, "Characteristics of activated carbon resulted from pyrolysis of the

oil palm fronds powder," *IOP Conf. Ser. Mater. Sci. Eng.*, vol. 309, no. 1, 2018, doi: 10.1088/1757-899X/309/1/012072.

[18] K. . Boadu, O. . Joel, D. . Essumang, and B. . Evbuomwan, "Comparative Studies of the Physicochemical Properties and Heavy Metals adsorption Capacity of Chemical Activated Carbon from Palm Kernel, Coconut and Groundnut Shells," *J. Appl. Sci. Environ. Manag.*, vol. 22, no. 11, p. 1833, 2019, doi: 10.4314/jasem.v22i11.19.

[19] L. Dong, W. Liu, R. Jiang, and Z. Wang, "Physicochemical and porosity characteristics of thermally regenerated activated carbon polluted with biological activated carbon process," *Bioresour. Technol.*, vol. 171, no. 1, pp. 260–264, 2014, doi: 10.1016/j.biortech.2014.08.067.

[20] E. Windiastuti, Suprihatin, Y. Bindar, and U. Hasanudin, "Identification of potential application of oil palm empty fruit bunches (EFB): A review," *IOP Conf. Ser. Earth Environ. Sci.*, vol. 1063, no. 1, 2022, doi: 10.1088/1755-1315/1063/1/012024.

[21] J. Wang, J. Xi, and Y. Wang, "Recent advances in the catalytic production of glucose from lignocellulosic biomass," *Green Chem.*, vol. 17, no. 2, pp. 737–751, 2015, doi: 10.1039/c4gc02034k.

[22] F. Dai, Q. Zhuang, G. Huang, H. Deng, and X. Zhang, "Infrared Spectrum Characteristics and Quantification of OH Groups in Coal," *ACS Omega*, vol. 8, no. 19, pp. 17064–17076, 2023, doi: 10.1021/acsomega.3c01336.

[23] T. G. Ambaye, M. Vaccari, E. D. van Hullebusch, A. Amrane, and S. Rtimi, "Mechanisms and adsorption capacities of biochar for the removal of organic and inorganic pollutants from industrial wastewater," *Int. J. Environ. Sci. Technol.*, vol. 18, no. 10, pp. 3273–3294, 2021, doi: 10.1007/s13762-020-03060-w.

[24] A. Elkhaleefa, I. H. Ali, E. I. Brima, A. B. Elhag, and B. Karama, "Efficient removal of Ni(II) from aqueous solution by date seeds powder biosorbent: Adsorption kinetics, isotherm and thermodynamics," *Processes*, vol. 8, no. 8, 2020, doi: 10.3390/PR8081001.

[25] A. Elkhaleefa, I. H. Ali, E. I. Brima, I. Shigidi, A. B. Elhag, and B. Karama, "Evaluation of the adsorption efficiency on the removal of lead(II) ions from aqueous solutions using Azadirachta indica leaves as an adsorbent," *Processes*, vol. 9, no. 3, 2021, doi: 10.3390/pr9030559.

[26] P. T. Tho *et al.*, "Enhanced simultaneous adsorption of As(iii), Cd(ii), Pb(ii) and Cr(vi) ions from aqueous solution using cassava root husk-derived biochar loaded with ZnO nanoparticles," *RSC Adv.*, vol. 11, no. 31, pp. 18881–18897, 2021, doi: 10.1039/d1ra01599k.

[27] P. Kumar, "Adsorption of Lead (II) Ions from Simulated Wastewater Using Natural Waste: A Kinetic, Thermodynamic and Equilibrium Study," *Environ. Prog. Sustain. Energy*, vol. 33, no. 3, pp. 55–64, 2014, doi: 10.1002/ep.

[28] E. Muindi, J. Mrema, E. Semu, P. Mtakwa, C. Gachene, and M. Njogu, "Phosphorus Adsorption and Its Relation with Soil Properties in Acid Soils of Western Kenya," *Int. J. Plant Soil Sci.*, vol. 4, no. 3, pp. 203–211, 2015, doi: 10.9734/ijpss/2015/13037.

[29] P. R. Rout, P. Bhunia, and R. R. Dash, "Modeling isotherms, kinetics and understanding the mechanism of phosphate adsorption onto a solid waste: Ground burnt patties," *J. Environ. Chem. Eng.*, vol. 2, no. 3, pp. 1331–1342, 2014, doi: 10.1016/j.jece.2014.04.017.

[30] M. Rashid, N. T. Price, M. Á. Gracia Pinilla, and K. E. O'Shea, "Effective removal of phosphate from aqueous solution using humic acid coated magnetite nanoparticles," *Water Res.*, vol. 123, pp. 353–360, 2017, doi: 10.1016/j.watres.2017.06.085.

[31] S. S. Mayakaduwa *et al.*, "Equilibrium and kinetic mechanisms of woody biochar on aqueous glyphosate removal," *Chemosphere*, vol. 144, pp. 2516–2521, 2016, doi: 10.1016/j.chemosphere.2015.07.080.

[32] R. Karunanithi *et al.*, "Sorption, kinetics and thermodynamics of phosphate sorption onto soybean stover derived biochar," *Environ. Technol. Innov.*, vol. 8, pp. 113–125, 2017, doi: 10.1016/j.eti.2017.06.002.

[33] K. W. Jung, M. J. Hwang, K. H. Ahn, and Y. S. Ok, "Kinetic study on phosphate removal from aqueous solution by biochar derived from peanut shell as renewable adsorptive media," *Int. J. Environ. Sci. Technol.*, vol. 12, no. 10, pp. 3363–3372, 2015, doi: 10.1007/s13762-015-0766-5.